Evaluation of a Long-Range Joint Acoustic Navigation / Thermometry System

Timothy F. Duda and Andrey K. Morozov
Applied Ocean Physics and Engineering Department
Woods Hole Oceanographic Institution
Woods Hole, MA 02543 USA

Bruce M. Howe
Applied Physics Laboratory, University of Washington
1013 NE 40th Street
Seattle, WA 98105-6698 USA

Michael G. Brown
Rosenstiel School of Marine and Atmospheric Science
University of Miami
4600 Rickenbacker Causeway, Miami, FL 33149

Kevin Speer and Peter Lazarevich
Department of Oceanography
Florida State University
Tallahassee, FL 32306-4230

Peter F. Worcester and Bruce D. Cornuelle
Scripps Institution of Oceanography
University of California at San Diego
9500 Gilman Drive
La Jolla, CA 92093-0230 USA

Abstract **– The conceptual architecture of an ocean acoustic system with the dual uses of submerged platform navigation and large-scale temperature measurement has been developed, and is described here. Swept FM signals would be used to synthesize short-duration pulses. A 50-Hz bandwidth is to be used, within the frequency range of 100 to 200 Hz. The potential performance of the system is discussed here. Navigation performance is compared with that of the currently used 1.6-Hz bandwidth RAFOS system. Thermometry performance can be evaluated using experiences with prior systems.**

I. INTRODUCTION

Low frequency (order hundreds of hertz) acoustical technology has been used for many decades to determine the positions of submerged passive current-following floats for studies of oceanic flow. The contemporary version of this is the RAFOS system [1]. During the same period, similar technology has been used to measure ocean temperature and current via very precise one-way and two-way acoustic travel time measurement, a practice called either tomography or thermometry, depending on whether images and mappings are sought, or simply measurements along a transect [2]. Here, the prospect of joining the two technologies into one system is discussed. We call this RAFOS-2. The anticipated performance of such a system is discussed and compared with previous implementations. Theoretical considerations and computer simulations of long-distance pulse propagation through ocean environments with multiple scales of sound-speed heterogeneity are employed.

Both functions of the system require pulse compression to improve signal to noise ratio at long distances. Phase-encoded binary maximal-length sequences have been used most often for tomography and propagation research applications, with as high a bandwidth as possible. Typically the quality factor Q is 2 to 4, with, for example, 37.5-Hz bandwidth at 75 Hz center frequency [3] and 100-Hz bandwidth at 250 Hz [2]. Linear frequency modulation (LFM) with differentiable phase, which is Doppler tolerant yet also suitable for tomography [4], has been used by RAFOS. The new system would use smoothly frequency modulated (FM) low-frequency signals (LFM or similar) for simultaneous navigation and thermometry, with the most precise long-term thermometry employing fixed paths between installations. Signals of 50-Hz bandwidth in the

1-4244-0115-1/06/$20.00 ©2006 IEEE

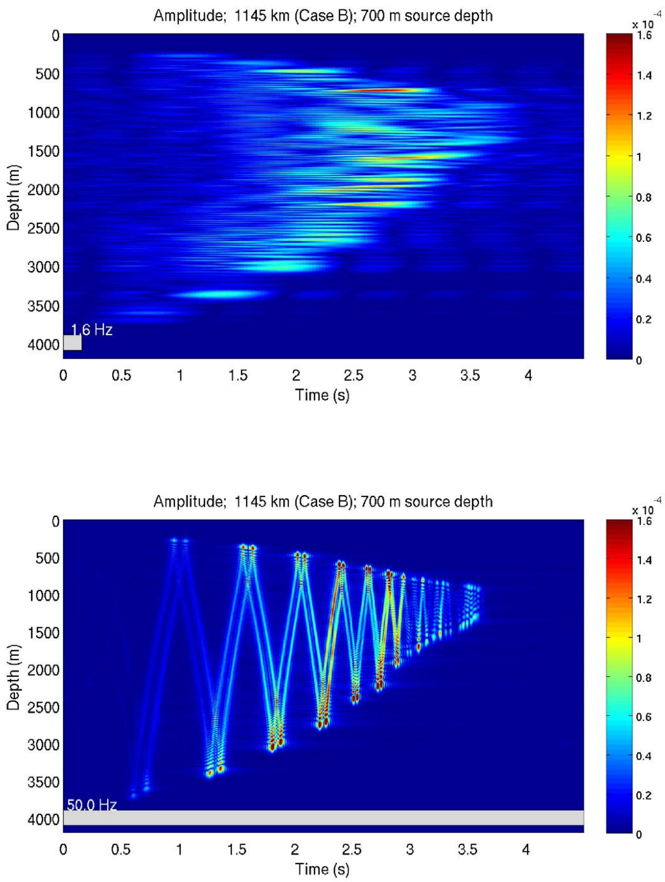

Figure 1. Properties of two types of signals transmitted along a northeasterly path from 15N 50W to 22N 42W in the Atlantic are compared. The source-receiver distance is 1145 km. The source depth is 700 m. (Upper panel) Baseband amplitude (amplitude of the complex envelope) of a pulse with 1.6-Hz bandwidth and 260-Hz center frequency is shown as a function of reduced time and depth. (Lower panel) As in the upper panel, except that the bandwidth has been increased to 50 Hz.

frequency range 100-200 Hz are suggested. This has been enabled by recent acoustic projector developments [5]. Such a system can be used to navigate drifting floats, gliders, profiling floats while submerged, and AUV's.

The RAFOS system uses eighty-second long linear FM signals of 1.5 Hz bandwidth centered near 260 Hz. It has been used for tracking floats for many decades, and its performance forms a benchmark for comparison. Typically, RAFOS is usable at distances exceeding 1800 km in temperate ocean regions. The wider bandwidth of the new signals would theoretically allow for more precise travel-time measurement, and thus more precise receiver localization. The lower frequency band of the new signals would reduce the effects of absorption, giving greater usable range. Furthermore, the increased bandwidth would concentrate the output of correlator detectors into sharper peaks in the time domain, providing further gain. On the other hand, the resolution of multipath that the new signals enable would reduce the energy in individual arrivals, serving to shorten the usable range. Experience with high-bandwidth tomography systems has illustrated these effects [2].

Tomography studies using wide-band signals have quantified many of the effects that limit system performance. Measured time series of travel times are combinations of the long-period ocean "weather" and "climate" signals of interest and aliased contributions from internal waves. The effects of internal waves are diminished at reduced acoustic frequency, known from previous work. Increased bandwidth may allow degrading effects of arrival structure uncertainty to be mitigated. The complicated structure of pulse arrival structures in the ocean waveguide, which will change with bandwidth, makes the implementation of a broader-band navigation/thermometry system an interesting scientific problem.

II. Ocean Impulse Response

The shapes of impulsive wavefronts, often represented by time-front diagrams, are complicated and well-known. They arise from the waveguide nature of the ocean [2]. The structure of a pulse from an actual acoustic system will be the convolution of two functions, the Fourier transform of the window function of frequency for the system, and the true impulse response. Fig. 1 shows band-limited pulse structures for a transmission path in the North Atlantic Ocean for systems with 1.6-Hz and 50-Hz bandwidth, respectively, computed with a PE code. The model range-dependent sound-speed environment does not include internal waves, which are known to smear out the impulse response [6]. Many multipath arrivals and many caustics can be seen in the wide-band result, which has a well-documented basic form. The most intense sections of the narrow-band time-front are associated with caustics, which are visible in the wide-band result. The association can be readily seen in a movie of the pulse form changing as a function of bandwidth.

The 1.6-Hz bandwidth result, corresponding to a pulse synthesized by matched-filtering a RAFOS signal, has intense sections that last about 0.5 s and that are intermittent in depth. Fig. 2 shows the matched-filter amplitude at 2000-m depth for each bandwidth. Approximately fifteen sharp arrivals are seen for the wide-band system, one for narrow-band. (Including internal waves may smear some of these together.) The wide-band prediction in the figure is similar to many pulses measured in the ocean [2]; the narrow-band result agrees with data from RAFOS floats which usually show one arrival, sometimes two or three.

III. Constraints on Tracking

Drifting floats with matched-filter receivers are routinely tracked over time. Trajectories can be computed on a ping-by ping localization basis, or with a Kalman filter using temporal sequences of signals. Constraints on tracking accuracy and precision are many. For the purposes of this paper, accuracy means freedom from absolute geographic position errors relative to the source network, and precision means freedom

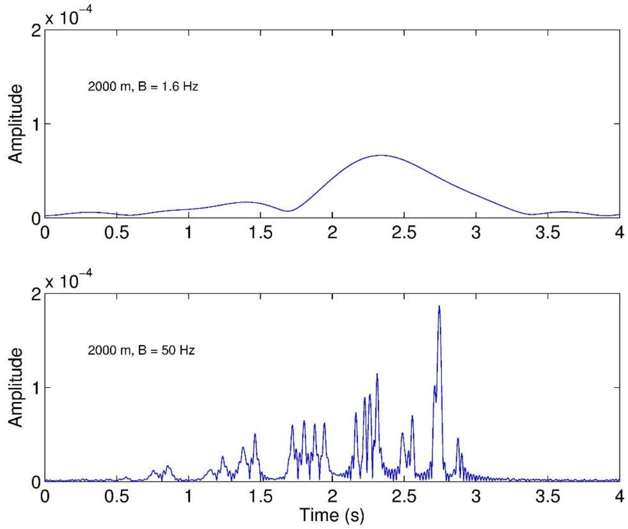

Figure 2. Slices through the Fig. 1 amplitudes at 2000 m depth. The result for bandwidth of 1.6 Hz is shown above, 50 Hz below.

from random high-frequency position errors. These errors can be estimated using residual travel times after localization.

After correcting source and receiver clocks, the major cause of inaccuracy is mismatch between model and actual ocean sound-speed structure along the acoustic paths. A model is required to convert travel-time to source/receiver distance. Long-period (weeks or greater) travel-time residuals for RAFOS floats, after localization, are typically one to three seconds, equivalent to 1.5 to 4.5 km location uncertainty.

Precision is restricted by at least three effects: Source motion, Doppler, and stochastic or quasi-steady variations of the arrival time of the signal peak used for localization. Two are system related, and the third can be interpreted in terms of the impulse response.

Source moorings can be pushed hundreds of meters laterally by currents, a process than can be measured and accounted for but is usually not. This can produce residuals of similar scale. The Doppler offset in arrival time for an LFM signal such as RAFOS is given by

$$\tau = -T\varepsilon/2 - \omega\varepsilon/b$$

where T is the signal duration, $\varepsilon = v/c$ is the scaled Doppler velocity, ω is the center frequency, and b is the sweep rate defined by signal phase $\theta(t) = bt^2/2 + \omega t$ [4]. The first term is related to an alteration of the duration of the arriving coded signal, and is equivalent to the average time shift of the entire waveform. The second term is related to the narrow-band Doppler shifted frequency. The second term is large for slow sweep rates. For slow-sweeping RAFOS signals, the second term can be as large as 1.0 s. The first term is negligible in comparison. Because of this, RAFOS tracking improves if Doppler offsets are estimated from sequential localizations and used to adjust travel times, in a bootstrap scenario. This procedure only guesses at the true Doppler shift because internal-wave effects on float velocity will be aliased. The new system can utilize CW tones along with the LFM so that the Doppler shift can be directly determined.

Uncertainty in the detail of impulse responses is an important limiting factor. The impulse response is sensitive to mesoscale features and internal wave features. Fig. 3 shows arrival times of signal peaks that might be used for localizing a RAFOS float. There is a clear variation with depth spanning about two seconds, which could possibly be estimated with theory, but there is also a random looking component to the pattern which has a roughly one-second spread within small depth intervals. This random timing variation will inevitably lead to float position uncertainty of the order of 1500 m.

Mathematically, the patterns in Fig. 2 are the results of convolution of the appropriate bandwidth-determined sinc functions (or related function for frequency tapering) with the impulse responses. The precise locations of caustics, which can dominate the results, are sensitive functions of the sound channel structure, and can vary at all time scales. Data show that intensity can vary strongly at periods as short as minutes, consistent with simulation of pulse propagation through evolving internal waves [7,8], which were not included in our simulations. Other work suggests that surface waves can also cause rapid fluctuations for surface-ducted environments. All of this is evidence that the depth-time coordinates of caustics may vary rapidly. Thus, instantaneous narrow-band arrival time realizations in the real ocean may be unpredictable.

IV. Tracking Benefits of Increased Bandwidth

The limitations of Doppler and pulse response on precision can be mitigated by increasing bandwidth to levels commonly used in many other ocean acoustic systems. First of all, a factor of twenty increase to 30 Hz bandwidth would reduce

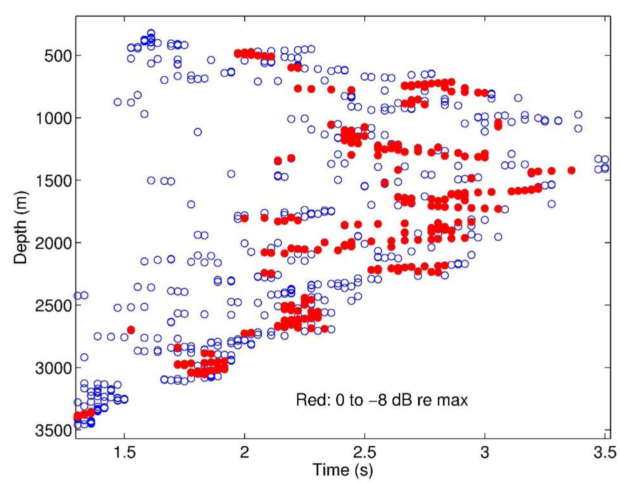

Figure 3. Arrival time of the peak signal at each depth is shown for the narrow-band pulse at the top of Fig. 1. Strong signals within 8 dB of the peak are shown in red, weaker signals in blue

Doppler effects to 5% of what they are for RAFOS. Next, increasing the bandwidth would allow the entire pulse response to be utilized. The bottom of Fig. 2 shows an arrival structure not unlike those commonly observed, which have been found to correspond well with modeled arrivals, and which have been found to be amenable to inversion [9]. The pattern of arrivals has much information encoded in the details such as the inter-group spacing and the spacing of arrivals within groups. These detailed arrival structures provide much more information about the source-receiver distance than does the single narrow-band arrival shown at the top of Fig. 2. An important factor is that with wide bandwidth the entire pattern is resolved, and intense features or caustics will not mask the less-intense features as occurs with the narrow bandwidth.

The precise times of the individual peaks will vary and some will be obscured because of internal waves [10], but individual realizations of the pattern (or an ensemble of a few) should constrain the source/receiver distance to within a few hundred meters even before applying inverse methods to improve the fit [11]. The estimate of a few hundred meters is based on experience in temperate mid-gyre areas, and may be optimistic for more dynamic areas with stronger eddies. Thus, the ability of wide-band signals to measure the arrival pattern should improve float localization above the narrow-band capability, perhaps reducing residuals (and float position error ellipses) to a few hundred meters, from 2 km or more.

Further gains may be possible using inversion techniques such as global search or linear methods to jointly obtain float locations and the intervening sound-speed structure [12]. The locations and the environment can not be unambiguously found from travel-time data alone. Precise navigation of sources can help by removing source locations from the set of unknowns. Sound-speed data from the floats and sources, nearby profiling floats, and data assimilative models can further constrain the inverse. There is a potential to obtain the sound-speed structure to an accuracy that will reduce the travel-time residuals to the noise level of a few milliseconds rms that stems from internal wave activity [10]. As a result, there is a potential to locate drifting floats to an accuracy of 50 m or less, equivalent to travel time residuals of 30 ms or less.

V. Thermometry

Long-term continuous measurement of average temperature (heat content) along gyre-scale or basin-scale acoustic paths has the potential to divulge important mechanisms in the global climate system. Monitoring acoustic pulse travel time between the source moorings, particularly if the mooring motion is monitored, can give very accurate measures of sound-speed conditions [2,13], the basis of thermometry. The difference between thermometry and tomography is one of detail: tomography systems intend to resolve detail within a measurement slice or volume, whereas thermometry systems intend to measure average temperature. Time series of travel time (or sound speed) can be converted to temperature by assuming constant salinity. Accuracy can be improved with timely monitoring of salinity, which has a minor effect [14]. Internal waves and mesoscale features will introduce variance into the records at high-frequency, but this should pose no difficulty with sufficient sampling. A small bias effect from waves and eddies explainable via Fermat's principle of least time should be approximately constant over time. Long climate-related time series will result. Note that the acoustic paths extend to great depth in the oceans, so that typically heat content from zero to 4500 m depth can be estimated. Using upper ocean records from other instruments, for example, fleets of profiling floats operating in the upper 1000 or 2000 m (depending on design), heat content in both the upper and lower oceans can be measured and distinguished.

VI. Apparatus

The first large-scale ocean acoustic tomography studies used 224-Hz and 400-Hz organ-pipe type resonator projectors (tube sources). Although these had a narrow resonance at the frequency having wavelength four times the resonator length, they did transmit sufficient energy over a large enough bandwidth to allow pulse compression. These sources had the advantage of being flooded, with no pressure-equalized enclosed portion, so they could be operated easily at any depth. Interestingly, these were based on designs used for SOFAR floats and moored RAFOS projectors. (SOFAR floats were drifting sources used for velocity studies, navigated by transmitting to fixed receivers. They were the predecessor to RAFOS floats, which operate inversely.) Later, other types of sources were used for tomography and thermometry, but most of these required pressure equalization and thus great mass, complexity and cost. Some were also less efficient than the tube sources.

A desire for greater simplicity, greater efficiency, and greater reproducibility of digital pulse synthesis behavior motivated research into an improved tube source design. The tight resonance of the organ pipes meant that source efficiency suffered at the edges of the band, so a new tunable design was developed and built [5]. The device is a tube resonator similar to the RAFOS and tomography sources, with tuning slots cut into the tubes. Mechanical opening and closing of the slots controls the resonance of the source, with Q of 100 and adjustment range approaching greater than one-half octave. The new design can send smoothly-modulated FM signals, including the simple LFM, by synchronously tuning the resonance to match the instantaneous frequency with a feedback system, thereby achieving maximum efficiency.

Fig. 4 is a schematic of the design. Fig. 5 is a photo. The first models operated in the band 200 to 300 Hz. The initial unit of the second generation is being built now. This will operate at 140 to 190 Hz.

Future plans are to push the design to operate at lower frequency. This can be accomplished without using unreasonably large ceramic transducers by using a tapered design rather than a tube. Finite element modeling has recently shown that a tube mated to an open cone at the end

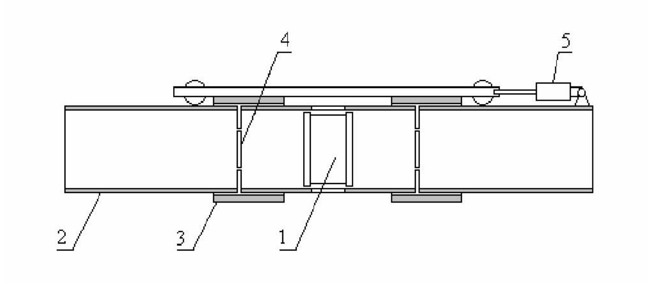

Figure 4. Resonator tube tunable projector. 1-symmetrical Tonpilz transducer; 2-resonator tube; 3-coaxial sleeves; 4-slots; 5-electrical actuator

(forming a horn) has very good characteristics. In addition, the modeling can be used to design the tuning slots.

VII. High-Precision Float Tracking

The potential ability of this system to locate isopycnal floats (floats with a feedback-controlled buoyancy adjuster maintaining position on a density surface) to the precision of 50 meters (Section IV) would allow field studies of small-scale Lagrangian motions in the ocean for the first time. The importance of processes at small scale (period shorter than a day or tidal cycle, for instance, and horizontal scale less than a few kilometers) to ocean dynamics has long been recognized. These motions have important implications in a variety of basic and applied oceanographic problems ranging from pollutant dispersal to maintenance of the ocean's thermohaline structure via coupling of isopycnal and diapycnal mixing. Eddy-diffusive isopycnal and diapycnal mixing processes occurring via motions on these scales transport suspended and dissolved substances, heat, and momentum across gradients. There are subsequent effects on transport and circulation patterns, ecosystems, and bio-geochemical fluxes. Studies of along-isopycnal diffusion and of internal tides (an important source of energy for across-isopycnal mixing), in particular, would be enabled.

While no direct measurements of small-scale Lagrangian motion have been made in the ocean interior, inferences pertaining to the importance of such measurements can be drawn from purposeful tracer release experiments. Data collected during the North Atlantic Tracer Release Experiment (NATRE) in 1992 suggest that isopycnal stirring at scales of order 1 km and smaller is poorly understood. Six months after injection of a chemical tracer on an isopycnal surface at approximately 300 m depth, the tracer patch was drawn into a filamentary form by the straining effect of the mesoscale field [15]. The area of the patch grew much greater than expected, and the main filament maintained a width of 3 km despite being elongated by the strain. This suggests an isopycnal eddy diffusivity of 2 $m^2\ s^{-1}$ at scales of 1 to 10 km. This value far exceeds that expected from internal-wave induced shear dispersion [16]. It has been suggested that potential vorticity-carrying vortical mode motions may play an important role in controlling the dispersion, with related work done by [17-19]. Clearly, the interpretation of dye distribution measurements would benefit from the high-resolution Lagrangian measurements that the proposed float system would provide. Purposeful tracer release measurements and high resolution Lagrangian measurements of the type potentially made possible by a RAFOS-2 system would be complementary.

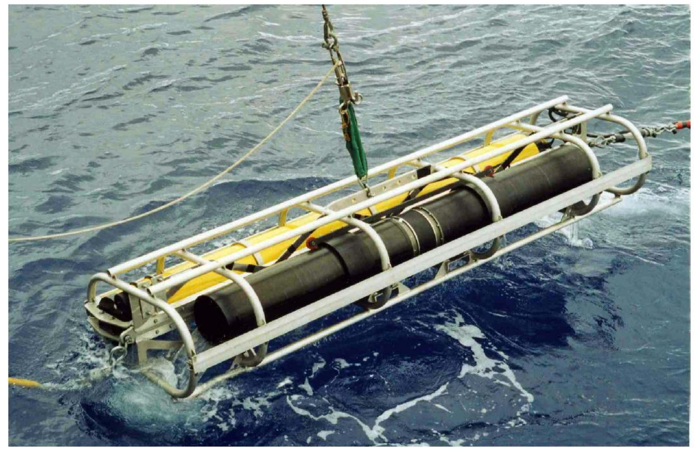

Figure 5. Photo of the resonator tube tunable projector being deployed at sea. The projector is mounted in an alloy cage. Approx. 750 kg, 3x1x0.5 m.

VIII. Summary

The anticipated performance of an envisioned RAFOS-2 float tracking and thermometry system has been presented. The system would operate with a bandwidth of order 50 Hz, at frequencies of 100 to 200 Hz. Using this frequency band should halve the effects of absorption, doubling the useful range and quadrupling the coverage area of each source in a navigation net or thermometry system, with respect to the RAFOS system which operates at 260 Hz.

The ability of the wide-band system to resolve the pulse response, not possible with RAFOS, would enable precise determination of the sound-speed field between the source and the receiver, improving accuracy and precision. This ability is implied by data obtained in the field over the prior few decades, and by theoretical studies. The system should be able to localize float position to a precision of 50 m or better.

Long-term continuous measurement of average temperature (heat content) along gyre-scale or basin-scale acoustic paths is also enabled by the system, in complete analogy with prior work, particularly that done in the North Pacific Ocean and the Mediterranean Sea [3,20,21].

Finally, a network of sources transmitting signals to many floats would form a network capable of mapping ocean eddies, or at a minimum, capable of computing meaningful 3-dimensional volumetric estimates of heat content. This technology may be useful to apply over the long-term to climate related studies. It is also uniquely suited to areas of seasonal or permanent ice cover, where floats can't be localized with GPS, although many aspects of sound propagation under ice remain to be studied [22].

ACKNOWLEDGMENT

Supporting grants from the Office of Naval Research and the National Science Foundation over the years for this area of research are gratefully acknowledged. Heather Furey and Amy Bower of WHOI provided informative RAFOS float travel-time residual data.

REFERENCES

[1] Rossby, T., D. Dorson, and J. Fontaine, "The RAFOS system," *J. Atmos. Oceanic Techn.*, vol. 3, pp. 672-679, 1986.

[2] Munk, W., P. Worcester, and C. Wunsch, *Ocean Acoustic Tomography*, Cambridge: Cambridge U.P., 1995.

[3] Worcester, P. F., B. D. Cornuelle, M. A. Dzieciuch, W. H. Munk, B. M. Howe, J. A. Mercer, R. C. Spindel, J. C. Colosi, K. Metzger, T. G. Birdsall and A. B. Baggeroer, "A test of basin-scale acoustic thermometry using a large-aperture vertical array at 3250-km range in the eastern North Pacific Ocean," *J. Acoust. Soc. Am.*, vol. 105, pp. 3185-3201, 1999.

[4] Duda, T. F., "Analysis of finite-duration wide-band frequency sweep signals for ocean tomography," *IEEE J. Oceanic Engineering*, vol. 18, pp. 87-94, 1993.

[5] Morozov, A. K., and D. C. Webb, D. C., "A sound projector for acoustic tomography and global ocean monitoring," *IEEE J. Oceanic Eng.*, vol. 28, pp.174-185, 2003.

[6] Colosi, J. A., S. M. Flatté and C. Bracher, "Internal-wave effects on 1000-km oceanic acoustic pulse propagation: Simulation and comparison with experiment," *J. Acoust. Soc. Am.*, vol. 96, 452-468, 1994.

[7] Simmen, J. A., S. M. Flatté, H. A. DeFerrari, H. Nguyen, and N. J. Williams, "Near-caustic behavior in a 270-km acoustical experiment," *J. Acoust. Soc. Am.*, vol. 105, pp. 3231-3244, 1999.

[8] Beron-Vera, F. J., M. G. Brown, J. A. Colosi, S. Tomsovic, A. L. Virovlyansky, M. A. Wolfson, and G. M. Zaslavsky, "Ray dynamics in a long-range acoustic propagation experiment," *J. Acoust. Soc. Am.*, vol. 114, pp. 1226-1242, 2003.

[9] Cornuelle, B. D., P. F. Worcester, J. A. Hildebrand, W. S. Hodgkiss Jr., T. F. Duda, J. Boyd, B. M. Howe, J. A. Mercer and R. C. Spindel, "Ocean acoustic tomography at 1000-km range using wavefronts measured with a large aperture vertical array," *J. Geophys. Res.*, vol. 98, pp. 16,365-16,377, 1993.

[10] Duda, T. F., S.M. Flatte', J.A. Colosi, B.D. Cornuelle, J.A. Hildebrand, W.S. Hodgkiss, Jr., P.F. Worcester, B.M. Howe, J.A Mercer, and R.C. Spindel, "Measured wave-front fluctuations in 1000-km pulse propagation in the Pacific Ocean," *J. Acoust. Soc. Am.*, vol. 92, pp. 939-955, 1992.

[11] Worcester, P. F., B. D. Cornuelle, J. A. Hildebrand, W. S. Hodgkiss Jr., T. F. Duda, J. Boyd, B. M. Howe, J. A. Mercer and R. C. Spindel, "A comparison of measured and predicted broadband acoustic arrival patterns in travel time-depth coordinates at 1000-km range," *J. Acoust. Soc. Am.*, vol. 95, pp. 3118-3128, 1994.

[12] Duda, T. F., R. A. Pawlowicz, J. F. Lynch and B. D. Cornuelle, "Simulated tomographic reconstruction of ocean features using drifting acoustic receivers and a navigated source," *J. Acoust. Soc. Am.*, vol. 98, pp. 2270-2279, 1995.

[13] Dushaw, B. D., B. M. Howe, J. A. Mercer, R. C. Spindel, A. B. Baggeroer, D. Menemenlis, C. Wunsch, T. G. Birdsall, K. M. C. Clark, J. A. Colosi, B. D. Cornuelle, M. Dzieciuch, W. Munk, et al., "Multimegameter-range acoustic data obtained by bottom-mounted hydrophone arrays for measurement of ocean temperature," *IEEE J. Ocean. Eng*., vol. 24, pp. 202-214, 1999.

[14] Dushaw, B. D., "Inversion of multimegameter-range acoustic data for ocean temperature," *IEEE J. Oceanic Engineering*, vol. 24, pp. 215-223, 1999.

[15] Ledwell, J. R., A. J. Watson and C. S. Law., "Mixing of a tracer in the pycnocline," *J. Geophys. Res.*, vol. 103, pp. 21,499-21,529, 1998.

[16] Young, W. R., P. B. Rhines and C. J. R. Garrett, "Shear-flow dispersion, internal waves and horizontal mixing in the ocean," *J. Phys. Oceanogr.*, vol. 12, pp. 515-527, 1982.

[17] Polzin, K., and R. Ferrari, "Isopycnal dispersion in NATRE," *J. Phys. Oceanogr.*, vol. 34, pp. 247-257, 2004.

[18] Sundermeyer, M. A. and J.R. Ledwell, "Lateral dispersion over the continental shelf: Analysis of dye-release experiments," *J. Geophys. Res.*, vol. 106, pp. 9,603-9,621, 2001.

[19] Sundermeyer, M. A., J. R Ledwell, N. S. Oakey and B. J. W. Greenan, "Stirring by small-scale vortices caused by patchy mixing," *J. Phys. Oceanogr.*, vol. 35, pp. 1245-1262, 2005.

[20] Howe, B. M., B. D. Cornuelle, B. D. Dushaw, M. A. Dzieciuch, D. Menemenlis, J. A. Mercer, W. H. Munk, R. C. Spindel, D. Stammer, P. F. Worcester, and M. Zarnetske, "Acoustic remote sensing of large-scale temperature variability in the North Pacific Ocean.," OCEANS'04, MTS/IEEE Techno-Ocean '04, Kobe, Japan, 1504–1506, 2004. [DOI: 10.1109/OCEANS.2004.1406343].

[21] Skarsoulis, E. K., U. Send, G. Piperakis, and P. Testor, "Acoustic thermometry of the western Mediterranean basin," *J. Acoust. Soc. Am.* vol. 116, pp. 790-798, 2004.

[22] Gavrilov, A. N., and P. N. Mikhalevsky "Low-frequency acoustic propagation loss in the Arctic Ocean: Results of the Arctic climate observations using underwater sound experiment," *J. Acoust. Soc. Am.*, vol. 119, pp. 3694-3706, 2006.